Shielded transient self-interaction of a bunch entering a circle from a straight path

R. Li, C. L. Bohn, and J. J. Bisognano
Thomas Jefferson National Accelerator Facility, 12000 Jefferson Ave., Newport News, VA 23606

ABSTRACT

Recent developments in electron-gun and injector technologies enable production of short (mm-length), high-charge (nC-regime) bunches. In this parameter regime, the curvature effect on the bunch self-interaction, by way of coherent synchrotron radiation (CSR) and space-charge forces as the beam traverses magnet bends, may cause serious emittance degradation. In this paper, we study an electron bunch orbiting between two infinite, parallel conducting plates. The bunch moves on a trajectory from a straight path to a circular orbit and begins radiating. Transient effects, arising from CSR and space-charge forces generated from source particles both on the bend and on the straight path prior to the bend, are analysed using Liénard-Wiechert fields, and their overall net effect is obtained. The influence of the plates on the transients is contrasted to their shielding of the steady-state radiated power. Results for emittance degradation induced by this self-interaction are also presented.

Keywords: coherent synchrotron radiation, space charge, free-electron laser, accelerator physics, Liénard-Wiechert potential, emittance, beam dynamics, wakefield, boundary problem

1. INTRODUCTION

When a short (mm-length) bunch with high-charge (nC-regime) is injected into magnetic bending systems, coherent synchrotron radiation (CSR) and space-charge interaction, due to the curvature of beam orbit, set up a wakefield across the bunch. This beam self-interaction will induce energy spread in the charged particles in the bunch, and may cause degradation of beam quality via the energy dependence of particle orbits in dispersive regions. Such possibility is of concern for various transport-lattice designs associated with free-electron lasers (FELs), including, for example, bunch-compressor chicanes preceding wigglers and recirculation loops associated with energy recovery. To circumvent this deleterious effect of curvature-induced self-interaction in lattice designs, one needs a thorough understanding of the phenomenon.

Almost all previous theoretical work on CSR has concerned its steady-state properties. Examples concerning steady-state CSR in free space include the frequency-domain and time-domain analyses by Schiff[1] and Derbenev, et al.,[2] respectively. Examples concerning steady-state CSR with shielding, i.e., in the presence of conducting walls, include the frequency-domain analyses by Nodvick and Saxon,[3] Warnock and Morton,[4] and Kheifets and Zotter,[5] and the time-domain analysis by Murphy, Krinsky, and Gluckstern.[6] Only recently have transients in finite-length magnetic bends begun to be considered, the principal example being the time-domain analysis of Saldin, et al.[7] concerning the transient interaction of a bunch with itself as it passes from a straight path into a circle in free space. These investigators showed that both space-charge forces originating from the straight path, and space-charge and CSR forces originating from the circle, make important contributions to the transient self-interaction.

In this paper, we generalize the theory of transient self-interaction in a magnetic bend by incorporating conducting walls to introduce shielding of CSR. Working in the time domain, we consider an electron bunch with a rigid-line-charge Gaussian distribution orbiting in the center plane between two infinite, parallel conducting plates. The bunch moves from a straight path to a circular orbit and begins radiating. Transient forces arising from source particles on the straight path (space charge) and on the circle (space charge and CSR) are calculated, and their net effects on beam energy spread and emittance growth are consequently obtained. For the characterization of the duration and magnitude of the transient effect, the power loss by a bunch due to this curvature effect is also analysed. All our results obtained in this paper can be reduced to those of Saldin, et al[7] in the free-space situation.

The presence of the two plates causes fields radiated from the bunch at an earlier time to bounce from plate to plate and eventually interact back with the bunch at a later time. The parallel-plate system is equivalent to an array of image bunches in free space moving simultaneously with the bunch in planes parallel to the plane of beam motion,

with alternating signs of charge, and spaced by the gap width of the two plates. The two systems are equivalent because they both satisfy the boundary condition at the plates and Maxwell's equations between the plates. This allows us to study the shielding of two conducting plates in terms of the interaction of the bunch with fields emitted by the image bunches.

2. LONGITUDINAL WAKEFIELDS ON THE BUNCH DUE TO CURVATURE-INDUCED SELF-INTERACTION

We start with the general Hamiltonian formalism for an electron with charge e:

$$H = c\sqrt{(\mathbf{P} - e\mathbf{A}/c)^2 + m^2c^2} + e\Phi, \tag{1}$$

where $\mathbf{p} = \mathbf{P} - e\mathbf{A}/c = \gamma m\mathbf{v}$ is the particle's kinetic momentum, in which $\mathbf{v}$ is its velocity, γ is the Lorentz factor; Φ and $\mathbf{A}$ are the scalar and vector electromagnetic potentials, respectively, on the electron arising from the interaction of an external field and the rest of the charge distribution. Given a rigid-line-charge bunch entering a circle from a straight path, the rate of change of the kinetic energy for an "observer" electron S, located on the bunch at the space-time coordinate $(\mathbf{r}, t)$, can be derived from the above Hamiltonian using $dH/dt = \partial H/\partial t$, which yields

$$mc^2\frac{d\gamma}{dt} = e\left[-\frac{d\Phi}{dt} + \frac{\partial}{\partial t}(\Phi - \boldsymbol{\beta}\cdot\mathbf{A})\right], \tag{2}$$

where the potentials Φ and $\mathbf{A}$ on electron S can be derived in terms of the potentials Φ_0 and $\mathbf{A}_0$ generated by a single "source" electron S' on the bunch:

$$[\Phi, \mathbf{A}](\mathbf{r}, t) = \int_{-\infty}^{\infty} [\Phi_0, \mathbf{A}_0](\mathbf{r}, t; s')\, n(s')ds' \tag{3}$$

where $n(s')$ is the line-density of the bunch, with s' denoting the distance of electron S' from the bunch center, and

$$[\Phi_0, \mathbf{A}_0](\mathbf{r}, t; s') = e\left[\frac{(1, \boldsymbol{\beta})}{(1 - \boldsymbol{\beta}\cdot\mathbf{n})R}\right]_{\text{ret}}, \qquad (\mathbf{R} = \mathbf{r} - \mathbf{r}'(t'), R = |\mathbf{R}|, \mathbf{n} = \mathbf{R}/R). \tag{4}$$

Here $\boldsymbol{\beta} = \mathbf{v}/c$, and the subscript "ret" in Eq. (4) imposes the retardation condition, which accounts for the nonzero time needed for the field emitted by S' at retarded space-time $(\mathbf{r}', t')$ to reach S at $(\mathbf{r}, t)$:

$$R = c(t - t'). \tag{5}$$

Since the trajectory $\mathbf{r}'(t')$ of S' is prescribed as a function of s', for given s', the retarded space-time of S' is uniquely determined by Eq. (5). One can also express Eqs. (2) and (4) by way of the longitudinal wakefield $E_\theta(\mathbf{r}, t)$ on electron S, which is on the circular orbit,

$$\begin{aligned} &mc^2\frac{d\gamma}{dt} = \beta ceE_\theta, \quad E_\theta(\mathbf{r}, t) = \int_{-\infty}^{\infty} ds' E_{\theta 0}(\mathbf{r}, t; s')\, n(s'), \\ &E_{\theta 0}(\mathbf{r}, t; s') = \frac{1}{\beta c}\left[-\frac{d\Phi_0}{dt} + \frac{\partial}{\partial t}(\Phi_0 - \boldsymbol{\beta}\cdot\mathbf{A}_0)\right] \end{aligned} \tag{6}$$

where $E_{\theta 0}$ is the single-particle longitudinal field exerted by S' on S.

It is shown in Eq. (6) that the single-particle field $E_{\theta 0}(\mathbf{r}, t; s')$ forms the basis of our wakefield analysis, which in turn is the foundation for the calculation of energy spread, emittance degradation, and the power loss by the beam due to its self-interaction. Since the geometric relation between S' and S incorporated in $E_{\theta 0}(\mathbf{r}, t; s')$ depends on whether the field is generated by S' from the straight path prior to the bend or from the circular orbit, in what follows we shall use the indices "(a)" and "(b)" to denote the cases when the source particle S' at retarded times t' is located on the straight path and the circle, respectively. To take into account the interaction of S from image charges due to the presence of the parallel plates, the source particle S' is allowed to have an offset z' perpendicular to the plane of the orbit. This will correspondingly affect the retardation times associated with image charges.

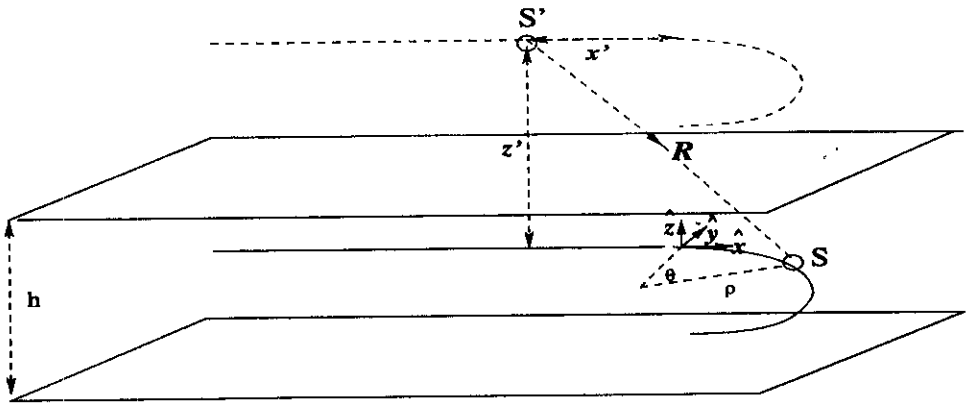

Figure 1. Interaction of S' on S, with S' on the straight path prior to the bend at the retarded time, and S on the circular orbit. The plate spacing is h, and the circle has radius ρ.

2.1. Case (a): S' on straight path at t', S on circle at t

As shown in Fig. 1, an observer electron S, at angle θ on the circle of radius ρ at time t, experiences a force generated from a source electron S' (which, in Fig. 1, is an image charge) at coordinate $\mathbf{r}' = (-x', 0, z')$ at time t' ($x' \geq 0$). With $t = 0$ being the moment when the bunch center enters the circle, the trajectories of S and S' are respectively described by

$$\begin{array}{ll} S : \rho\theta = s + \beta ct & \text{(circular path)} \\ S' : -x' = s' + \beta ct' & \text{(straight path)} \end{array} \tag{7}$$

In the coordinate system $(\hat{\mathbf{x}}, \hat{\mathbf{y}}, \hat{\mathbf{z}})$, depicted in Fig. 1, the vector $\mathbf{R}$ from S' to S is

$$(R_x, R_y, R_z) = (\rho\sin\theta + x', \rho\cos\theta - \rho, z'), \quad \text{and} \quad R = \sqrt{R_x^2 + R_y^2 + R_z^2}. \tag{8}$$

The interaction from S' to S obeys the retardation relation in Eq. (5) with R given in Eq. (8). Also, in this coordinate system, the factor $(1 - \boldsymbol{\beta}\cdot\mathbf{n})R$ in the single-particle potentials given in Eq. (4) can be written as

$$(1 - \boldsymbol{\beta}\cdot\mathbf{n})R = \sqrt{R_x'^2 + R_\perp^2/\gamma^2} \qquad (R_\perp^2 \equiv R_y^2 + R_z^2,\ R_x' \equiv R_x - \beta R,\ \boldsymbol{\beta}_{ret} = (\beta, 0, 0)). \tag{9}$$

Notice R_x' is the distance from S_p' to S projected on the $\hat{\mathbf{x}}$-direction, with S_p' denoting the position of S' at time t were it to continue executing uniform linear motion at all retarded times $t' \leq t$. Upon substracting the two formulas in Eq. (7) and using Eq. (5), one gets

$$R_x' = \rho(\Delta\phi + \sin\theta - \theta), \qquad (\Delta\phi = \Delta s/\rho,\ \Delta s = s - s') \tag{10}$$

where $\Delta\phi$ is the angular intra-bunch distance between S and S' in the bunch frame.

The longitudinal electric field due to single-particle interaction can be obtained from Eq. (6), where the functional dependence of Φ_0 and $\mathbf{A}_0$ for given (θ, t) on s' is through $\Delta\phi$ in Eqs. (9) and (10). This yields

$$E_{\theta 0}^{(a)} = -\frac{\partial V^{(a)}}{\partial \Delta s}, \quad \text{with} \quad V^{(a)}(\theta, \Delta s, z') = V_0^{(a)} + (\Phi_0 - \boldsymbol{\beta}\cdot\mathbf{A}_0)^{(a)}, \tag{11}$$

where

$$V_0^{(a)} = \mathcal{V}_0^{(a)}(\theta, \infty, z') - \mathcal{V}_0^{(a)}(\theta, \Delta s, z'), \quad \text{with} \quad \mathcal{V}_0^{(a)}(\theta, \Delta s, z') = e\frac{(1 - \cos\theta) - R_y R_x' \sin\theta/R_\perp^2}{\sqrt{R_x'^2 + R_\perp^2/\gamma^2}}, \tag{12}$$

and

$$(\Phi_0 - \boldsymbol{\beta}\cdot\mathbf{A}_0)^{(a)} = e\frac{1 - \beta^2\cos\theta}{\sqrt{R_x'^2 + R_\perp^2/\gamma^2}}. \tag{13}$$

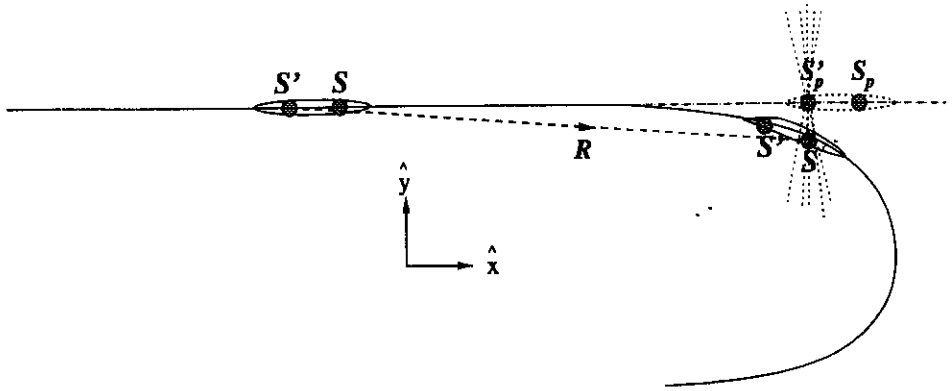

Figure 2. The field generated by S' is a pancake shaped disc associated with its pseudo present location S'_p at time t, which shines right on the observer electron S when $R'_x = 0$ as S enters into the bend.

Here $V_0^{(a)}$ is derived from $d\Phi_0^{(a)}/dt$ in Eq. (6): $\partial V_0^{(a)}/\partial \Delta s = d\Phi_0^{(a)}/\beta c dt$.

To confirm the validity of the above expressions, we carry out the differentiation in Eq. (11) using Eqs. (12) and (13), and obtain

$$E_{\theta 0}^{(a)} = e\frac{\gamma R'_x \cos\theta + \gamma |R_y| \sin\theta}{(\gamma^2 R'^2_x + R_\perp^2)^{3/2}}, \tag{14}$$

which agrees with the longitudinal component of the following Lienard-Wiechert field on S generated by S'

$$\mathbf{E} = e\left[\frac{\mathbf{n}-\boldsymbol{\beta}}{\gamma^2(1-\boldsymbol{\beta}\cdot\mathbf{n})^3 R^2}\right]_{\rm ret} + \frac{e}{c}\left[\frac{\mathbf{n}\times(\mathbf{n}-\boldsymbol{\beta})\times\dot{\boldsymbol{\beta}}}{(1-\boldsymbol{\beta}\cdot\mathbf{n})^3 R}\right]_{\rm ret}. \tag{15}$$

Here, because of the uniform motion of S' on the straight path, the second term in Eq. (15) vanishes, and the interaction from S' to S is solely due to space charge.

From Eq. (14), if $\gamma R'_x \gg R_\perp$, we have $E_{\theta 0} \propto \gamma^{-2}$, a result similar to the inertial space-charge interaction. However, when $R'_x = 0$, we have $E_{\theta 0} = e\gamma R_y \sin\theta / R_\perp^3 \propto \gamma$. Hence when $\gamma \gg 1$, the space-charge field from S' to S is an impulse-like function of R'_x. The corresponding physical picture is depicted in Fig. 2 for the interaction of S' with S in free space, where the electric field at time t generated by S' at retarded time t' is a pancake-shaped disc associated with S'_p— the pseudo present location of S'. For given intra-bunch spacing Δs, as S enters into the bend, it moves from the side of the disc to a point when the disc-shaped field shines right on S when $R'_x = 0$, or $\Delta\phi = \theta - \sin\theta$. We will show that in this case the straight path has a non-trivial space-charge effect on the particles moving in the bend, which is comparable to that of CSR on the circle.

2.2. Case (b): S' on circle at t', S on circle at t

The motions of S and S' are now described by

$$S : \rho\theta = s + \beta ct, \qquad S' : \rho\theta' = s' + \beta ct'. \tag{16}$$

To obtain the dependence of the lab-frame interaction angle $\Delta\theta = \theta - \theta'$ on the intra-bunch angular spacing $\Delta\phi = \Delta s/\rho$ of the two causally related particles, we subtract the two equations in Eq. (16), and use the retardation relation in Eq. (5) to obtain the transcendental equation through which $\Delta\theta$ is uniquely determined by $\Delta\phi$ for given ρ and z':

$$\rho\Delta\theta = \rho\Delta\phi + \beta R, \qquad R = \sqrt{[2\rho\sin(\Delta\theta/2)]^2 + z'^2}. \tag{17}$$

In the following we consider only the forward radiation in that $\Delta\theta \geq 0$. In free space, for which $z' \equiv 0$, the causality condition in Eq. (17) gives

$$\Delta\theta = 4\mathrm{sh}[(1/3)\mathrm{sh}^{-1}(3\gamma^3\Delta\phi/2)]/\gamma. \tag{18}$$

For image charges, with $z' \neq 0$, one can approximate Eq. (17) by

$$\Delta\theta^4 - (24\Delta\phi)\Delta\theta - 12(z'/\rho)^2 = 0, \qquad \left(\frac{12^{\frac{1}{2}}}{\gamma} \text{ and } 12^{\frac{1}{4}}\Delta\phi \ll \Delta\theta \ll 2\gamma^2\Delta\phi \text{ and } \frac{\gamma z'}{\rho}\right) \tag{19}$$

which has the solution

$$\Delta\theta = \frac{\Delta\theta_0}{3^{1/4}}\left[\sqrt{\sqrt{\frac{\mathrm{sh}\eta}{\mathrm{sh}(\eta/3)}} - \mathrm{sh}\frac{\eta}{3}} + \frac{\Delta\phi}{|\Delta\phi|}\sqrt{\mathrm{sh}\frac{\eta}{3}}\right] \quad \text{for} \quad \eta \equiv \mathrm{sh}^{-1}\left[\frac{9\Delta\phi^2}{2(z'/\rho)^3}\right],\ \Delta\theta_0 \equiv (12)^{1/4}(z'/\rho)^{1/2}. \tag{20}$$

The linear region of Eq. (20) corresponds to $\eta \ll 1$, whence it reduces to

$$\Delta\theta \simeq \Delta\theta_0\left[1 + (3/4)^{1/4}\Delta\phi(z'/\rho)^{-3/2}\right] \quad \text{for} \quad \eta \ll 1. \tag{21}$$

with $\Delta\theta_0$ the value of $\Delta\theta$ when $\Delta\phi = 0$. When $\eta \gg 1$, $\Delta\theta$ in Eq. (20) behaves as

$$\Delta\theta \simeq 2(3\Delta\phi)^{1/3}H(\Delta\phi) \quad \text{for} \quad \eta \gg 1, \tag{22}$$

with $H(x)$ denoting the Heaviside step function. The transition from behavior in Eq. (21) to that in Eq. (22) occurs in the intermediate range $\eta \sim 1$.

When both S' and S move on the circle, one can show that $d\Phi_0^{(b)}/dt = 0$, and consequently the single particle field in Eq. (6) becomes

$$E_{\theta 0}^{(b)} = -\frac{dV^{(b)}}{d\Delta s}, \quad \text{with} \quad V^{(b)}(\Delta s, z') = (\Phi_0 - \boldsymbol{\beta}\cdot\mathbf{A}_0)^{(b)}. \tag{23}$$

The factor $(1 - \boldsymbol{\beta}\cdot\mathbf{n})R$ in Φ_0 and $\mathbf{A}_0$ of Eq. (6) can be written as

$$(1 - \boldsymbol{\beta}\cdot\mathbf{n})R = R - \beta\rho\sin\Delta\theta. \tag{24}$$

With $\Delta\theta$ implicitly given in Eq. (17), we have

$$V^{(b)}(\Delta s, z') = e\frac{(1 - \beta^2\cos\Delta\theta)}{R(\Delta\theta, z') - \beta\rho\sin\Delta\theta}, \tag{25}$$

where $R(\Delta\theta, z')$ is given in Eq. (17). One can write $E_{\theta 0}^{(b)}$ in Eq. (23) explicitly by expressing

$$\frac{d}{d\Delta s} = \left(\frac{d\Delta\theta}{\rho d\Delta\phi}\right)\frac{d}{d\Delta\theta}, \tag{26}$$

with $(d\Delta\theta/d\Delta\phi)$ obtained using Eq. (17), and show that $E_{\theta 0}^{(b)}$ thus obtained from Eq. (23) agrees with that given in Eq. (15).

2.3. Longitudinal Wakefield on S from the Whole Bunch

In this section we derive the longtitudinal wakefield on a single electron S, which is on the circular orbit, by integrating the single-particle field generated from the whole bunch distribution. Part of the field is generated by source particles in the bunch when they were on the straight path before the bend, and part by source particles already on the circular orbit. To remove the singularity due to the line-bunch model when S and S' overlap in free space (when $z' = 0$), and to see the curvature effect of the circular motion of S, we calculate the residual longitudinal wakefield exerted by the whole bunch on S:

$$\hat{E}_\theta(\mathbf{r}, t) = \int_{-\infty}^{\infty} ds'\,\hat{E}_{\theta 0}(\mathbf{r}, t, s')\,n(s'), \quad \text{with} \quad \hat{E}_{\theta 0} = E_{\theta 0} - E_{s0}. \tag{27}$$

Here $E_{\theta 0}$ is given in Eq. (6), and E_{s0} is the inertial single-particle space-charge field from S' to S when the bunch moves on a straight path with constant velocity $\mathbf{v} = \beta c$:

$$E_{s0} \equiv -\frac{dV_s}{d\Delta s}, \qquad V_s(\Delta s, z') = \frac{e}{\gamma^2\sqrt{\Delta s^2 + z'^2/\gamma^2}}. \tag{28}$$

The corresponding residual potentials are

$$\hat{V}^{(a,b)} = V^{(a,b)} - V_s. \tag{29}$$

When calculating $\hat{E}_\theta$ on S in Eq. (27), we use $\hat{E}^{(a)}_{\theta 0} = E^{(a)}_{\theta 0} - E_{s0}$ for $\hat{E}_{\theta 0}$ when the source electron S' is on the straight path, and $\hat{E}^{(b)}_{\theta 0} = E^{(b)}_{\theta 0} - E_{s0}$ for $\hat{E}_{\theta 0}$ when S' is on the circular orbit. Consequently one gets

$$\hat{E}_\theta(\theta, s, z') = \hat{E}^{(a)}_\theta + \hat{E}^{(b)}_\theta, \tag{30}$$

with

$$\begin{aligned} \hat{E}^{(a)}_\theta &= \int_{\Delta s_t(\theta,z')}^{\infty} \hat{E}^{(a)}_{\theta 0}(\theta, \Delta s, z'))n(s - \Delta s)d\Delta s, \\ \hat{E}^{(b)}_\theta &= \int_{\Delta s_0(z')}^{\Delta s_t(\theta,z')} \hat{E}^{(b)}_{\theta 0}(\Delta s, z')n(s - \Delta s)d\Delta s. \end{aligned} \tag{31}$$

The integration limit $\Delta s = \Delta s_t(\theta, z')$ in Eq. (31) is the transition point from cases (a) to (b) when S' is at the entrance of the arc, namely, $\theta' = x' = 0$. Using Eq. (17) with $\Delta\theta = \theta - \theta' = \theta$, we have

$$\Delta s_t(\theta, z') = \rho\theta - \beta\sqrt{[2\rho\sin(\theta/2)]^2 + z'^2}. \tag{32}$$

The transition between forward and backward radiation occurs at $\Delta\theta = 0$. From Eq. (17) this corresponds to

$$\Delta s_0(z') = -\beta|z'|. \tag{33}$$

In Eq. (31) the negligible contribution to $\hat{E}^{(b)}_\theta$ from $\Delta s \in (-\infty, \Delta s_0)$ through backward radiation is not included.

Furthermore, one can show that the limiting behavior of $V^{(b)}$ at $\Delta s \to \Delta s_0$ is

$$V^{(b)}(s \to \Delta s_0, z') = \begin{cases} \dfrac{e}{\gamma^2\Delta s_0} & (z' = 0, \Delta s_0 \to 0, \Delta\theta \to \dfrac{\Delta\phi}{1-\beta}) \\ \dfrac{e}{\gamma^2|z'|} & (z' \neq 0, \Delta s_0 = -\beta|z'|, \Delta\theta = 0) \end{cases}, \tag{34}$$

which leads to $\hat{V}^{(b)}(\Delta s_0, z') = 0$. Also one has $\hat{V}^{(a)}(\theta, \Delta s, z')|_{\Delta s \to \infty} = 0$. With these limits, and using Eqs. (11), (23) and (28) for the expression of $E^{(a)}_{\theta 0}$, $E^{(b)}_{\theta 0}$, and E_{s0}, respectively, one can integrate Eq. (31) by parts, and rewrite Eq. (30) for the longitudinal wakefield on S from the bunch as

$$\hat{E}_\theta(\theta, s, z') = E^{(a)}_0 + E^{(a)} + E^{(b)} \tag{35}$$

with

$$E^{(a)}_0 = [\hat{V}^{(a)}(\theta, \Delta s_t, z') - \hat{V}^{(b)}(\Delta s_t, z')]n(s - \Delta s_t), \tag{36}$$

$$E^{(a)} = \int_{\Delta s_t(\theta,z')}^{\infty} d\Delta s\, \hat{V}^{(a)}(\theta, \Delta s, z')\frac{dn(s - \Delta s)}{d\Delta s}, \tag{37}$$

$$E^{(b)} = \int_{\Delta s_0(z')}^{\Delta s_t(\theta,z')} d\Delta s\, \hat{V}^{(b)}(\Delta s, z')\frac{dn(s - \Delta s)}{d\Delta s}. \tag{38}$$

Due to the continuity of potentials at $\theta' = 0$, or $\Delta s = \Delta s_t \equiv \Delta s_t(\theta, z')$,

$$(\Phi_0 - \boldsymbol{\beta}\cdot\mathbf{A}_0)^{(a)}|_{\Delta s_t} = (\Phi_0 - \boldsymbol{\beta}\cdot\mathbf{A}_0)^{(b)}|_{\Delta s_t}, \tag{39}$$

we can write Eq. (36) as

$$E_0^{(a)} = V_0^{(a)}(\theta, \Delta s_t, z')n(s - \Delta s_t). \tag{40}$$

We now move on to calculate each term in Eq. (35). First we consider $E_0^{(a)}$ in Eq. (40), where $V_0^{(a)}$ given in Eq. (12) can be simplified as

$$V_0^{(a)}(\theta, \Delta s_t, z') = -\frac{e}{\rho}\frac{|R_y|}{R + R_x}, \qquad (R_x = \rho\sin\theta \ \text{ at } \ x' \doteq 0,\ R = \sqrt{R_x^2 + R_\perp^2}), \tag{41}$$

which reduces to a simpler expression for free-space interaction ($z' = 0$):

$$V_0^{(a)}(\theta, \Delta s_t, 0) = -\frac{e}{\rho}\tan(\theta/4). \tag{42}$$

Secondly we study $E^{(a)}$ in Eq. (37), where the potential $\hat{V}^{(a)}(\theta, \Delta s, z')$ can be explicitly written as

$$\hat{V}^{(a)}(\theta, \Delta s, z') = e\frac{|R_y|\sin\theta}{R_\perp^2}\left[1 - \frac{R_x' - \frac{R_\perp^2\cos\theta}{\gamma^2|R_y|\sin\theta}}{\sqrt{R_x'^2 + R_\perp^2/\gamma^2}}\right] - V_s, \tag{43}$$

In the limit $\gamma \to \infty$ Eq. (43) cuts off at $R_x' = 0$, or at $\Delta s = \Delta s_c$:

$$\hat{V}^{(a)} \simeq \begin{cases} 0 & (R_x' > 0, \ \text{ or } \ \Delta s > \Delta s_c) \\ V_{ac} & (R_x' \le 0, \ \text{ or } \ \Delta s \le \Delta s_c) \end{cases}, \tag{44}$$

where

$$V_{ac}(\theta, z') = \frac{2e|R_y|\sin\theta}{R_\perp^2}, \quad \text{ and } \quad \Delta s_c = \rho(\theta - \sin\theta). \tag{45}$$

Since $\hat{E}_{\theta 0}^{(a)} = -\partial\hat{V}^{(a)}/\partial\Delta s$, the step function behavior of $\hat{V}^{(a)}$ in Eq. (44) depicts the strong δ-function-like Coulomb interaction from S' to S when the pancake like Coulomb field carried by the pseudo particle S_p', as introduced earlier in Sec. 2.1, shines right on the electron S when $R_x' = 0$. Comparing Δs_c in Eq. (45) and Δs_t in Eq. (32), one has $\Delta s_c > \Delta s_t$ for $\gamma\theta > 1$. Therefore the integration range for $E^{(a)}$ in Eq. (37) is from Δs_t to Δs_c, leading to

$$E^{(a)}(\theta, s, z') \simeq V_{ac}(\theta, z')[n(s - \Delta s_c) - n(s - \Delta s_t)]. \tag{46}$$

Lastly we look at $E^{(b)}$ in Eq. (38) with $V^{(b)}$ given in Eq. (25). In free space ($z' = 0$), one can replace Δs in V_s of Eq. (28) by $\Delta\theta$ using the retardation relation in Eq. (18), and get

$$\hat{V}^{(b)}(\Delta s, 0) \simeq e\frac{2\gamma^2\alpha(2 + \gamma^2\alpha^2)}{\rho(1 + \gamma^2\alpha^2)(3 + \gamma^2\alpha^2)} \qquad (\alpha = \Delta\theta/2), \tag{47}$$

which has the following asymptotic behavior

$$\hat{V}^{(b)}(\Delta s, 0) \simeq \begin{cases} \dfrac{4e\gamma^2\alpha}{3\rho} \approx \dfrac{4e\gamma^4\Delta\phi}{3\rho} & (\gamma\alpha \ll 1, \ \alpha \to \gamma^2\Delta\phi) \\ \dfrac{2e}{\rho\alpha} \approx \dfrac{2e}{\rho(3\Delta\phi)^{1/3}} & (\gamma\alpha \gg 1, \ \alpha \to (3\Delta\phi)^{1/3}) \end{cases}. \tag{48}$$

For a Gaussian bunch with charge density function

$$n(s) = \frac{N}{\sqrt{2\pi}\sigma_s}e^{-s^2/2\sigma_s}, \tag{49}$$

where N is the total number of electrons in the bunch, and σ_s is the root-mean-square (rms) bunch length, we combine Eq. (48) with Eq. (38) to obtain the free-space ($z' = 0$) steady-state ($\theta_0 = \infty$) wakefield across the bunch

$$\hat{E}_\theta^{\text{free}}(s) \equiv \hat{E}_\theta(\theta = \theta_0 + s/\rho, s, z')|_{\theta_0 \to \infty, z' = 0}. \tag{50}$$

Using the $\gamma^3\Delta\phi \gg 1$ approximation for $\hat{V}_\delta$ in Eq. (48), we obtaine

$$\hat{E}_\theta^{\rm free}(s) = \frac{2Ne}{3^{1/3}\sqrt{2\pi}\rho^{2/3}\sigma_s^{4/3}} \int_0^\infty d\phi_1 \frac{(\phi_s - \phi_1)}{\phi_1^{1/3}} e^{-(\phi_s-\phi_1)^2/2}, \qquad (\phi_s = s/\sigma_s,\ \phi_1 = \Delta s/\sigma_s) \tag{51}$$

a result in agreement with Derbenev, et al.[2]

It is now straightforward to incorporate two infinite parallel plates spaced by the gap width h, with the bunch moving on the plane centered between the plates, by considering the array of image charges that comove with the bunch in the planes $z' = \pm nh$ in free space, in which $n \neq 0$ denotes the image bunch. The total longitudinal force on the electron S from all the image bunches is thus obtained from $\hat{E}_\theta$ in Eq. (35),

$$\hat{E}_\theta^{\rm sh}(\theta_0, s; h) = \sum_{n=-\infty}^{\infty} (-)^n \hat{E}_\theta(\theta = \theta_0 + s, s, nh), \tag{52}$$

in which $\theta_0 = \beta ct$ is the angle of the bunch center in the arc. Eq. (52) is the principal result of this paper, for it constitutes the starting point for calculating bend-induced energy spread, which in turn causes degradation in transverse emittance. An example of wakefield using parameters in Jefferson Lab' infrared FEL,[8] where a bunch with 1 mm bunch length and 40 MeV energy enters into an arc with 1 m radius, was calculated using Eq. (52) for varying gap width h between the two conducting plates. The transient development of the wakefield from small amplitude at $\theta_0 = 5°$ to the steady-state behavior at $\theta_0 = 90°$ is depicted in Figs. 3(a), 3(b) and 3(c), respectively. These figures show that the wakefields obtained for plate spacing $h = 0.05$ m approximately agree with the free-space wakefields. The shielding effect can be seen for $h = 0.02$ m, when the wakefields have smaller amplitude and higher freqeucy component compared to those of free-space case.

3. POWER LOSS DUE TO BUNCH SELF-INTERACTION

For characterizing the duration and magnitude of the transients, we turn to calculating the shielded power loss $\hat{P}^{\rm sh}(\theta_0; h)$ of the bunch induced by its self-interaction. This is obtained by integrating the kinetic energy loss of a single electron over the portion of the bunch lying on the circle:

$$\hat{P}^{\rm sh}(\theta_0; h) = \hat{P}(\theta_0, 0) + 2\sum_{n=1}^{\infty}(-)^n \hat{P}(\theta_0, nh), \tag{53}$$

with $\hat{P}(\theta_0, nh)$ the power loss of bunch, when the bunch center is at θ_0, due to its interaction with the nth image bunch obtained from $\hat{E}_\theta(\theta, s, nh)$ in Eq. (52), i.e.,

$$\hat{P}(\theta_0, nh) = -\beta ce \int_{-\theta_0}^{\infty} ds \hat{E}_\theta(\theta = \theta_0 + s/\rho, s, nh) n(s). \tag{54}$$

Here the integration spans $\theta \geq 0$, or $s/\rho \geq -\theta_0$. The free-space power loss is the $n = 0$ term in Eq. (53):

$$\hat{P}^{\rm free}(\theta_0) = \hat{P}(\theta_0, 0). \tag{55}$$

When the whole bunch is well into the bend, $\theta_0 \gg \sigma_s/\rho$, the lower limit $-\theta_0$ in Eq. (54) effectively becomes $-\infty$, and one has $\theta \approx \theta_0$. Upon defining the the following functions

$$f(\Delta s) \equiv \int_{-\infty}^{\infty} n(s) n(s - \Delta s) ds, \qquad g(\Delta s) \equiv df(\Delta s)/d\Delta s, \tag{56}$$

and denoting $\Delta s_i^{(n)}(\theta_0) = \Delta s_i(\theta_0, nh)$, we have from Eq. (54)

$$\hat{P}(\theta_0, nh) \simeq P_0^{(a)}(\theta_0, nh) + P^{(a)}(\theta_0, nh) + P^{(b)}(\theta_0, nh), \tag{57}$$

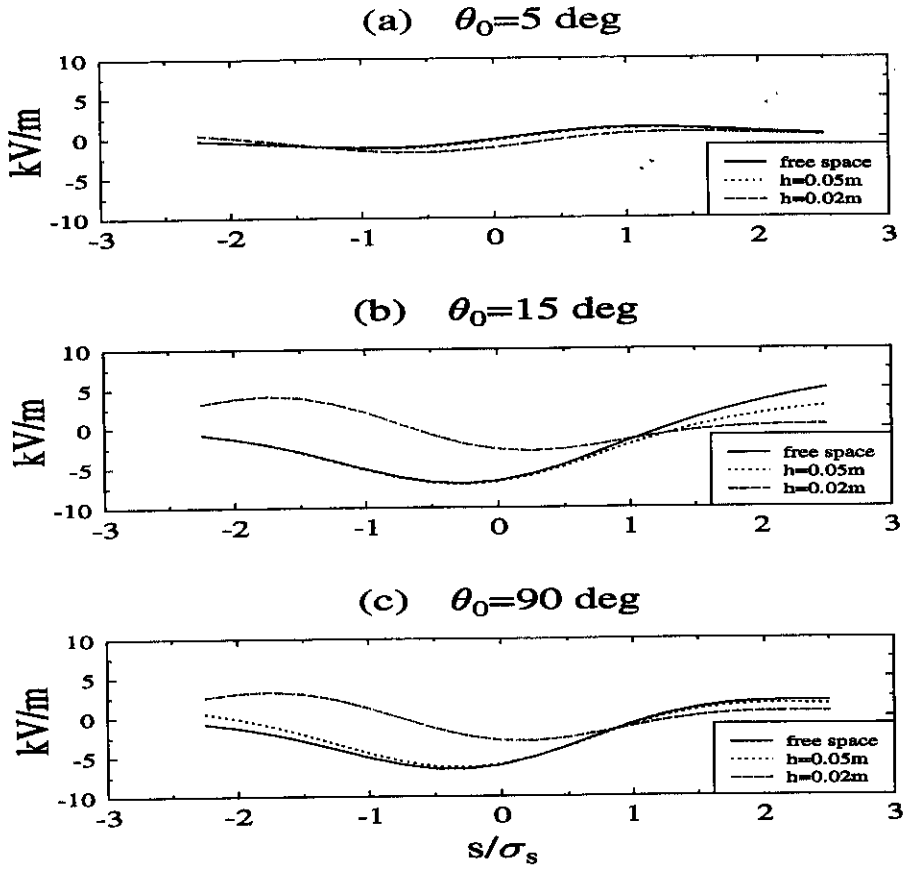

Figure 3. Longitudinal wakefield $\hat{E}_\theta^{\rm sh}(\theta_0, s; h)$, as given in Eq. (52), across the bunch set by the CSR and space-charge-induced beam self-interaction, when the beam center is at each of the following angle into the arc: (a) $\theta_0 = 5°$, (b) $\theta_0 = 15°$, and (c) $\theta_0 = 90°$. Here $\rho = 1$ m, $\sigma_s = 1$ mm, $I_{\rm peak} = 36$ A, and $E = 40$ MeV. The interaction saturates to steady state at case (c).

where each term in Eq. (57) is mapped to the terms in Eq. (35):

$$P_0^{(a)}(\theta_0, nh) = -\beta ce V_0^{(a)}[\theta_0, \Delta s_t^{(n)}(\theta_0), nh] f(\Delta s_t^{(n)}(\theta_0)), \tag{58}$$

$$P^{(a)}(\theta_0, nh) = -\beta ce V_{ac}(\theta_0, nh)[f(\Delta s_c) - f(\Delta s_t^{(n)})]|_{\theta=\theta_0}, \tag{59}$$

$$P^{(b)}(\theta_0, nh) = -\beta ce \int_{\Delta s_0(nh)}^{\Delta s_t^{(n)}(\theta_0)} d\Delta s \hat{V}^{(b)}(\Delta s, nh) g(\Delta s). \tag{60}$$

Here Eq. (58) is obtained from Eq. (40), Eq. (59) from Eq. (46), and Eq. (60) from Eq. (38).

3.1. Power Loss in Free Space for a Gaussian Bunch

Having developed the above tools, we first study the free-space power loss in Eq. (55) based on Eq. (57) with $n = 0$. For a Gaussian distribution given in Eq. (49), the functions $f(\Delta s)$ and $g(\Delta s)$ in Eq. (56) are

$$f(\Delta s) = \frac{N^2 e^{-\Delta s^2/4\sigma_s^2}}{2\sqrt{\pi}\sigma_s}, \qquad g(\Delta s) = -\frac{N^2 \Delta s\, e^{-\Delta s^2/4\sigma_s^2}}{4\sqrt{\pi}\sigma_s^3}. \tag{61}$$

For $\theta_0 \ll 1$ and $n = 0$, we have $\Delta s_t, \Delta s_0$ and Δs_c in Eqs. (58), (59) and (60) respectively as

$$\Delta s_t(\theta_0, 0) = \rho\theta_0^3/24, \quad \Delta s_0(0) = 0, \quad \Delta s_c(\theta_0) = \rho\theta_0^3/6, \tag{62}$$

by using Eqs. (32), (33) and (45). We now proceed to calculate each term in Eq. (57) with $n = 0$. The first term $P_0^{(a)}(\theta_0, 0)$ can be obtained using Eqs. (58) and (42):

$$P_0^{(a)}(\theta_0, 0) \simeq \frac{\beta c (Ne)^2}{\rho \sigma_s} \frac{\tan(\theta_0/4)}{2\sqrt{\pi}} e^{-[\Delta s_t(\theta_0, 0)]^2/2\sigma_s^2}. \tag{63}$$

Using Eq. (45) with $|R_\perp| = |R_y| \simeq \rho\theta_0^2/2$, the second term $P^{(a)}(\theta_0, 0)$ in Eq. (57) is obtained from Eq. (59) with $n = 0$:

$$P^{(a)}(\theta_0, 0) \simeq \frac{\beta c (Ne)^2}{\sqrt{\pi}\sigma_s \rho} \frac{2}{\theta_0} [e^{-[\Delta s_t(\theta_0, 0)]^2/2\sigma_s^2} - e^{-[\Delta s_c(\theta_0)]^2/2\sigma_t^2}]. \tag{64}$$

Inspection of Eqs. (63) and (64) shows that both $P_0^{(a)}(\theta_0, 0)$ and $P^{(a)}(\theta_0, 0)$ are transient functions of θ_0. The two functions both increase from zero at the entrance of the bend $\theta_0 = 0$, rise to their peak values, and decrease to negligible magnitude at $\theta_0 \sim \theta_{0t}$, with

$$\Delta s_t(\theta_{0t}, 0) = 2\sigma_s, \quad \text{or} \quad \theta_{0t} = 2(6\sigma_s/\rho)^{1/3}. \tag{65}$$

Notice that $P_0^{(a)}(\theta_0, 0)$ is about θ_0^2 times smaller compared to $P^{(a)}(\theta_0, 0)$. For the transient region discussed above, with $\sigma_s \ll \rho$, we have $\theta_0^2 \ll 1$. Therefore $P_0^{(a)}(\theta_0, 0)$ is negligible compared to $P^{(a)}(\theta_0, 0)$. The peak of the latter function is located at $\theta_0 \simeq \theta_{0c}$, where

$$P^{(a)}(\theta_{0c}, 0) \simeq \frac{\beta c (Ne)^2}{\sqrt{\pi}\sigma_s \rho} \frac{1.5}{\theta_{0c}} \qquad (s_c(\theta_{0c}) = 2\sigma_s \quad \text{or} \quad \theta_{0c} = (12\sigma_s/\rho)^{1/3}). \tag{66}$$

We now study $P^{(b)}(\theta_0, 0)$ in Eq. (57) by analysing the potential $\hat{V}^{(b)}(\theta_0, 0)$ in Eq. (60). As shown in Eq. (47) for free space, the potential $\hat{V}^{(b)}$ vanishes for the immediate-neighbor ($\alpha = \Delta\theta/2 = 0$) interaction, and reaches its peak value when $\alpha = \alpha_p$, or $\Delta\phi = \Delta\phi_p$ by solving Eq. (17), where $d\hat{V}^{(b)}/d\alpha|_{\alpha=\alpha_p} = 0$,

$$\hat{V}^{(b)}|_{\Delta\phi_p} \simeq 0.76 e\gamma/\rho, \qquad (\alpha_p \simeq 1.2/\gamma, \Delta\phi_p = 1.8\gamma^{-3}). \tag{67}$$

Combining the asymptotic behavior for $\hat{V}^{(b)}$ at $\gamma^3\Delta\phi \gg 1$ given by Eq. (48), we can write the factor $\hat{V}^{(b)}(\Delta s)\Delta s$ in the integrand of Eq. (60) as

$$\hat{V}^{(b)}(\Delta s)\Delta s \simeq e \begin{cases} 1.4\gamma^{-2} & (\Delta\phi = \Delta\phi_p) \\ 1.4\Delta\phi^{2/3} & (\Delta\phi \gg \gamma^{-3}) \end{cases}, \tag{68}$$

which is much smaller at $\Delta\phi = \Delta\phi_p$ than at $\Delta\phi \gg \gamma^{-3}$. Thus the energy-dependent peak $\hat{V}^{(b)}|_{\Delta\phi_p}$ is suppressed by Δs and has negligible contribution to $P^{(b)}(\theta_0, nh)$. This allows us to use the asymptotic behavior of $\hat{V}^{(b)}$ at $\Delta\phi \gg \gamma^{-3}$ in Eq. (60) to get

$$P^{(b)}(\theta_0, 0) \simeq \frac{\beta c (Ne)^2}{(6\rho^2\sigma_s^4)^{1/3}\sqrt{\pi}} \gamma[5/6, [s_t(\theta_0, 0)]^2/4\sigma_s^2], \tag{69}$$

where $\gamma[\nu, x]$ is the incomplete Gamma function. The formation angle for the radiated power to saturate to steady state, $\theta_0 = \theta_{0f}$, corresponds to the time for the head of the bunch to see photons emitted at the entrance of the bend by the tail of the bunch, namely

$$\Delta s_t(\theta_{0f}, 0) = 4\sigma_s, \quad \text{or} \quad \theta_{0f} \simeq 2(12\sigma_s/\rho)^{1/3}. \tag{70}$$

Note that both $P^{(a)}(\theta_{0c}, 0)$ in Eq. (66) and $P^{(b)}(\theta_0, 0)$ in Eq. (69) have the parameter dependence $(\rho^2\sigma_s^4)^{-1/3}$, indicating the straight-path contribution to transient bunch self-interaction is as significant as that of CSR. Since $P^{(a)}(\theta_0, 0)$ damps to zero at $\theta_0 \geq \theta_{0t}$, after a formation length ($\theta_0 \geq \theta_{0f} \geq \theta_{0t}$) one gets the steady-state power loss

$$\hat{P}^{\text{free}}(\infty) \simeq P^{(b)}(\theta_0 > \theta_{0f}, 0) \simeq \frac{\beta c (Ne)^2}{(\rho^2\sigma_s^4)^{1/3}} \frac{3^{1/6}}{2\pi} [\Gamma(2/3)]^2, \tag{71}$$

in agreement with Schiff.[1]

3.2. Power Loss due to Interaction with Far Away Image Charges

For image bunches $z' = nh$ far enough away, the beam cannot see the detailed distribution of the image bunch, and it interacts with the distant image bunches as if they were point charges. This happens when Eq. (21) reduces to

$$\Delta\theta(\Delta s) \simeq \Delta\theta_0 \quad (\sigma_s/\rho \ll (nh/\rho)^{3/2}), \tag{72}$$

for $|\Delta s| \leq 4\sigma_s$, so in Eq. (60) we have $\hat{V}^{(b)}(\Delta s, nh) \simeq \hat{V}^{(b)}(0, nh)$. In this case, $\Delta s_0(nh) \gg \sigma_s$. Hence, the limit $\Delta s_0(nh)$ in Eq. (60) is equivalent to $-\infty$ as seen by the bunch distribution, and Eq. (60) becomes

$$P^{(b)}(\theta_0, nh) \simeq -\beta ce\hat{V}^{(b)}(0, nh)\int_{-\infty}^{\Delta s_i^{(n)}} g(\Delta s)d\Delta s \simeq -\beta ce\hat{V}^{(b)}(\Delta s_i^{(n)}, nh)f(\Delta s_i^{(n)}), \tag{73}$$

where the approximation $\hat{V}^{(b)}(\Delta s_i^{(n)}, nh) \simeq \hat{V}^{(b)}(0, nh)$ is used. The total power loss due to the interaction of the nth image bunch with the bunch itself is $\hat{P}(\theta_0, nh)$ in Eq. (57). Summing up $P_0^{(a)}$, $P^{(a)}$ and $P^{(b)}$ given in Eqs. (58), (59) and (73), we find that the terms which are functions of $\Delta s_i^{(n)}$ cancel due to the continuity of the potentials as given in Eq. (39). Therefore, one has for a Gaussian bunch

$$\hat{P}(\theta_0, nh) \simeq -\beta ceV_{ac}(\theta_0, nh)f(\Delta s_c) \tag{74}$$

$$= -\frac{2\beta c(Ne)^2 \sin^2(\theta_0/2)\sin\theta_0}{\pi^{1/2}\sigma_s\rho[4\sin^4(\theta_0/2) + (nh/\rho)^2]} e^{-\Delta s_c(\theta_0)^2/2\sigma_s^2}, \qquad (\sigma_s/\rho \ll (nh/\rho)^{3/2}) \tag{75}$$

where $\hat{P}(\theta_0, nh)$ rises from zero value at the entrance of the bend $\theta_0 = 0$, and drops to zero value for $\theta_0 > \theta_{0c}$ when $\Delta s_c(\theta_0) > 2\sigma_s$. The peak value of $\hat{P}(\theta_0, nh)$ decreases with increasing n as expected. The fact that $\hat{P}(\theta_0, nh)$ in Eq. (75) is transient is consistent with the present understanding of shielding, namely, if the two parallel plates are separated by spacing $\Delta_n = nh$ with $\sigma_s/\rho \ll (\Delta_n/\rho)^{3/2}$, the contribution of the image bunches at $z' = \pm nh$ to steady-state shielding is negligible.

3.3. Power Loss in General Cases

The power loss obtained from Eq. (57), normalized by the free-space steady-state power loss $\hat{P}^{\text{free}}(\infty)$ in Eq. (71), is displayed in Fig. 4, with numerical integration applied for Eq. (60). Here we use parameters $\rho = 1$ m and $\sigma_s = 1$ mm, typical values in the recirculating accelerator that will drive Jefferson Lab's infrared FEL (the IR Demo).[8] The dotted curve is the transient power loss of the bunch in free space, $\hat{P}(\theta_0, 0)/\hat{P}^{\text{free}}(\infty)$, which rises from zero loss and saturates to steady state. The other curves in Fig. 4 pertain to the presence of parallel conducting plates. The solid curve corresponds to $h = 5$ cm, a typical pipe size in the IR Demo. This spacing is relatively large so as to avoid beam loss, whereas it provides little shielding of the self-interaction. Stronger shielding can be obtained for narrower gap size with fixed bunch length, as indicated by the dashed curve corresponding to $h = 2$ cm. In this case the steady-state power loss is 25% of the free-space value, in agreement with results obtained by power-spectrum analysis as reflected in Fig. 4 of Ref. [9].

4. EMITTANCE GROWTH DUE TO BUNCH SELF-INTERACTION

The calculation of emittance growth follows directly from the equation of motion. As an over-simplified model of beam dynamics, in this section we assume $\sigma_r/\sigma_s \ll (\rho/\sigma_s)^{1/3}$ when the rigid-line-charge model is valid,[2] and consider only the emittance growth as a result of the longitudinal wakefield discussed in the previous section. A complete picture of beam dynamics requires 3-D self-consistent simulation which takes into account the transverse beam size as well as the transverse force on the beam. We are presently engaged in developing such a simulation and will report it in future papers. Nevertheless, the simple model provides a tool for benchmarking the wakefield calculation for an accurate simulation treatment, as well as the lowest order of beam dynamics due to curvature-induced self-interaction.

Here we consider the beam motion as it enters into the bend at $t = 0$. To first order in deviation from the design orbit, the equation of motion for a particle in the relativistic bunch is

$$\frac{d^2x}{dt^2} + \omega_0^2 x = \frac{\rho\omega_0^2}{\beta_0^2\gamma_0}[\gamma_1(s, 0) + \Delta\gamma(s, t)], \tag{76}$$

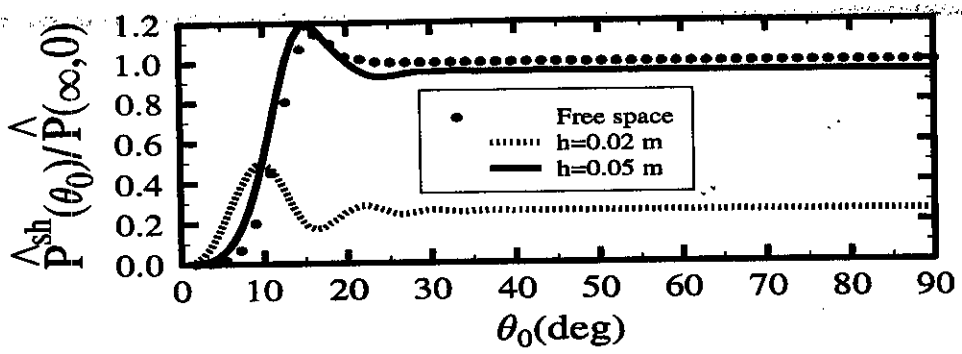

Figure 4. Transient power loss of a bunch, due to curvature-induced self-interaction in the presence of parallel plates, with $\rho = 1$ m, $\sigma_s = 1$ mm, $E = 40$ MeV, and various plate spacings.

in which x is the offset from the design orbit in the bend plane, $\gamma_1(s,0)mc^2$ is the initial energy offset from the design energy $\gamma_0 mc^2$, with $\beta_0 = \sqrt{1-\gamma_0^{-2}}$, and $\Delta\gamma(s,t)$ is the energy change induced by space charge and CSR:

$$\Delta\gamma(s,t)mc^2 = e\int_0^t E_\theta(s,t')\,v dt'. \tag{77}$$

Solving Eq. (76) for $\beta_0 \simeq 1$ using Green's theorem yields

$$\begin{bmatrix} x(s,t) \\ x'(s,t) \end{bmatrix} = M\left[\begin{pmatrix} x(s,0) \\ x'(s,0) \end{pmatrix} + \begin{pmatrix} \Delta x(s,t) \\ \Delta x'(s,t) \end{pmatrix}\right] + D\frac{\gamma_1(s,0)}{\gamma_0}, \tag{78}$$

where the prime denotes differentiation with respect to $\rho\omega_0 t$, and M and D are the transport matrix and dispersion vector for the bend, which are, respectively,

$$M = \begin{bmatrix} \cos\omega_0 t & \rho\sin\omega_0 t \\ -\rho^{-1}\sin\omega_0 t & \cos\omega_0 t \end{bmatrix}, \; D = \begin{bmatrix} \rho(1-\cos\omega_0 t) \\ \sin\omega_0 t \end{bmatrix}. \tag{79}$$

In Eq. (78) the space charge and the CSR induced dispersive offset and angle are, respectively,

$$\begin{bmatrix} \Delta x(s,t) \\ \Delta x'(s,t) \end{bmatrix} = \int_0^t \omega_0 dt' \begin{bmatrix} -\rho\sin\omega_0 t' \\ \cos\omega_0 t' \end{bmatrix} \frac{\Delta\gamma(s,t')}{\gamma_0}. \tag{80}$$

The normalized emittance is obtained from the determinant of the second moment matrix

$$[\epsilon(t)/\gamma_0]^2 = \begin{vmatrix} \langle(\delta x)^2\rangle & \langle\delta x\delta x'\rangle \\ \langle\delta x\delta x'\rangle & \langle(\delta x')^2\rangle \end{vmatrix}, \quad \text{with} \quad \begin{matrix} \delta x = x(s,t) - \langle x(s,t)\rangle, \\ \delta x' = x'(s,t) - \langle x'(s,t)\rangle, \end{matrix} \tag{81}$$

where the notation $\langle\rangle$ stands for taking average over the distribution. We now define the initial second moment as

$$\sigma_{x_0}^2 = \langle[\delta x(s,0)]^2\rangle,\; \sigma_{x_0'}^2 = \langle[\delta x'(s,0)]^2\rangle,\; \sigma_{x_0x_0'}^2 = \langle\delta x(s,0)\delta x'(s,0)\rangle, \tag{82}$$

and the CSR-induced second moment as

$$\sigma_{\Delta x}^2 = \langle(\Delta x - \langle\Delta x\rangle)^2\rangle,\; \sigma_{\Delta x'}^2 = \langle(\Delta x' - \langle\Delta x'\rangle)^2\rangle,\; \sigma_{\Delta x\Delta x}^2 = \langle(\Delta x - \langle\Delta x\rangle)(\Delta x' - \langle\Delta x'\rangle)\rangle. \tag{83}$$

With the initial emittance defined as ϵ_0: $\epsilon_0 \equiv \epsilon(t=0)$, we obtain the final emittance as

$$\epsilon = \sqrt{\epsilon_0^2 + \Delta\epsilon^2}, \tag{84}$$

where the emittance growth term is

$$(\Delta\epsilon/\gamma_0)^2 = [\sigma^2_{\Delta x}\sigma^2_{\Delta x'} - (\sigma^2_{\Delta x\Delta x'})^2] + (\sigma^2_{x_0}\sigma^2_{\Delta x'} + \sigma^2_{x'_0}\sigma^2_{\Delta x} - 2\sigma^2_{x_0x'_0}\sigma^2_{\Delta x\Delta x'}) + [...]. \tag{85}$$

The last term in Eq. (85) is related to the initial energy spread, which has zero contribution to $\Delta\epsilon$ at the end of an achromatic bending system where the dispersion vector D vanishes. When the term $\sigma^2_{x_0}\sigma^2_{\Delta x'}$ dominates in Eq. (85), the emittance growth is dominated by the CSR-induced dispersive deflection, one then has

$$\Delta\epsilon \simeq \gamma_0\sigma_{x0}\sigma_{\Delta x'}, \tag{86}$$

with σ_{x0} the initial transverse rms size of the beam at the entrance of the bend, and $\sigma_{\Delta x'}$ the CSR-induced rms transverse deflection.

As a simple example, we assume the wakefield across the bunch takes its free-space steady-state form everywhere inside the bend by neglecting the transient behavior before it saturates to steady state. Using Eqs. (51) and (77), one has

$$\Delta\gamma(s,t) = \kappa\omega_0 t g(s), \tag{87}$$

where by denoting $I_{\rm peak} = Nec/\sigma_s$ as the peak current, $I_A = mc^3/e$ the Alfven current, and $\phi_s = \sigma_s/\rho$, we have

$$\kappa = \frac{2}{3^{1/3}\sqrt{2\pi}}\left(\frac{\rho}{\sigma_s}\right)^{1/3}\frac{I_{\rm peak}}{I_A}, \qquad g(s) = \int_0^\infty d\phi_1 \frac{(\phi_s-\phi_1)}{\phi_1^{1/3}} e^{-(\phi_s-\phi_1)^2/2}. \tag{88}$$

As a result, the CSR-induced dispersive angular offset in Eq. (80) is

$$\Delta x' = (\omega_0 t\sin\omega_0 t + \cos\omega_0 t - 1)g(s)/\gamma_0. \tag{89}$$

Because $\sqrt{\langle[g(s)]^2\rangle - \langle g(s)\rangle^2} \simeq 0.4$, the free-space steady-state emittance growth given by Eq. (86) is

$$\Delta\epsilon = 0.4\kappa\,\sigma_{x0}(\omega_0 t\sin\omega_0 t + \cos\omega_0 t - 1). \tag{90}$$

5. CONCLUSION

In summary, we have calculated analytically the wakefield on the bunch due to self-interaction, and the corresponding power loss by the bunch, induced by the curvature effect, as a bunch enters from a straight path to a bend in the presence of conducting plates. Our results show that space charge from the straight path prior to the bend induces transients in the bunch self-interaction with magnitudes comparable to that from CSR. Also, it is shown that the interaction of the bunch with the nth image bunch, for $\sigma_s/\rho \ll (nh/\rho)^{3/2}$, has only transient effects on the total power loss of the bunch. The wakefields on the bunch due to self-interaction, as given in Sec. 2, are foundation for the energy-spread calculation, from which the emittance growth induced by the curvature effect can be obtained. The study of the actual beam dynamics under such self-interaction requires three-dimensional self-consistent simulation. Nevertheless, many features of the curvature-induced beam self-interaction, such as the interplay of the transient space-charge effect from the straight path prior to the bend and transient CSR from the circular orbit, and the shielding by the plates in light of the interaction of the bunch with image bunches, are revealed via the rigid-line-charge model applied in this analysis.

ACKNOWLEDGEMENTS

This work was supported by the U.S. Dept. of Energy under Contract No. DE-AC05-84ER40150.

REFERENCES

1. L. I. Schiff, Rev. Sci. Instr., **17**, 6-14, (1946).
2. Ya. S. Derbenev, J. Rossbach, E. L. Saldin, and V. D. Shiltsev, DESY Report No. TESLA-FEL-95-05, 1995(unpublished).
3. J. S. Nodvick and D. S. Saxon, Phys. Rev., **96**, 180 (1954).
4. R. L. Warnock and P. Morton, Part. Accel. **25** 1990.
5. S. A. Kheifets and B. Zotter, CERN SL-95-92 (AP), 1995.
6. B. Murphy, S. Krinsky, and R. L. Gluckstern, BNL-63090, (1996).
7. E. L. Saldin, E. A. Schneidmiller, and M. V. Yurkov, DESY-TESLA-FEL-96-14, (1996).
8. C. L. Bohn, Proceedings of the Particle Accelerator Conference, Vancouver, 1997.
9. R. Li, C. L. Bohn, and J. J. Bisognano, Proceedings of the Particle Accelerator Conference, Vancouver, 1997.